© 2018 IJSRST | Volume 4 | Issue 2 | Print ISSN: 2395-6011 | Online ISSN: 2395-602X
Themed Section: Scienceand Technology

NiO/YSZ Composite as a Precursor Material to SOFC Anodic Application

V. Mohanta, S. Otta and B. K. Roul*
Institute of Materials Science, Planetarium Building, Acharya Vihar, Bhubaneswar, Odisha, India

ABSTRACT

The conventional solid state reaction route is used to prepare ceramic composite from commercially available high-purity NiO (Aldrich, 99.99%) and YSZ (Aldrich, 99.9%) powders. Composites were characterized using X-ray diffraction (XRD), field emission scanning electron microscopy (FESEM) techniques. The NiO/YSZ composites were found to be in crystalline form with homogeneous mixture of YSZ and NiO phases. Impedance measurements and analysis were performed over a frequency range 1 kHz to 2 MHz at different temperatures. Conductivity in various temperature and different nickel contents were also studied which established the fact that the development of NiO/YSZ composite showed remarkable anodic properties which are highly suitable to be used as a precursor material for solid oxide fuel cell (SOFC).

Keywords: Solid state reaction route, NiO/YSZ composite, electrical properties, SOFC

I. INTRODUCTION

Solid oxide fuel cells (SOFCs) are solid-state electrochemical devices that convert chemical energy in fuels (H_2 and Hydrocarbons etc) directly into electrical energy with high efficiency [1]. Now a day, SOFCs have received more attention due to not only its high conversion efficiency but also high flexibility to various fuels (H_2, CH_4, etc) and low pollution emission [2]. In general, SOFCs consist of three main parts: a dense electrolyte between two porous electrodes (anode and cathode). Ni doped yttria stabilized zirconia (Ni/YSZ) is the most widely used anode material for SOFCs due to its high catalytic activity of H_2 oxidation, high mechanical/chemical stability at high temperature, long term reliability, low cost and their compatibility with most electrolytes and interconnect materials [3]. The electrochemical reaction inside the anode is supposed to occur around the triple-phase boundary (TPB) where the fuel gas, Ni and YSZ phase meet [4]. The presence of Ni serves as an excellent catalyst for the electrochemical oxidation of hydrogen whereas the YSZ provides necessary framework for the dispersion of Ni particles as well as offers ionic contribution to the overall conductivity, which broadens the TPB [5].

Since polarization resistance of Ni/YSZ is strongly influenced by its TPB [6], a reduction of polarization resistance of the anode may be attributed to a longer TPB, which enhances the electrochemical reaction [7]. Moreover, polarization resistance of the anode depends on both Ni content and its micro structure [7]. So, to have a potential anode for SOFC applications a finer micro structure along with uniform distribution of Ni, YSZ and pores in the anode is essential [8], which yields an improved electrochemical performance.

In this research work, NiO/YSZ composite was prepared by conventional solid state reaction route. Appropriate amount of zinc was used here as pore former. The composites were sintered at 1350^{0}C for 5 hours. The aim of the present paper is to look into anodic behaviour along with mechanism involved in our sample. We investigated the effect of both Ni

contents and temperature on the electrical properties of as prepared composite. Finally, our preparation method yielded a potential precursor for SOFC anode. Moreover, reduction of NiO/YSZ composites is essential in order to enhance the anodic performance.

II. METHODS AND MATERIAL

Most common method used for synthesizing the polycrystalline solids is the direct reaction, in the solid state, of a mixture of solids as starting materials. Ceramic composite samples were prepared with the traditional solid state reaction route. High-purity NiO (Aldrich, 99.99%) and YSZ (Aldrich, 99.9%) powders with different Ni wt% (Ni: 10 wt%, 20 wt%, 30 wt%, 40 wt%) were taken separately. As per Ni wt%, hereafter the composite samples will be termed as S10, S20, S30 and S40. NiO and YSZ powders are mixed thoroughly using agate mortar and pestle for two hour. Mixed powders were calcined in air at 600 ^{0}C for 3 h followed with mild manual crushing by agate mortar. The procedure was repeated for three times in order to achieve a homogeneous mixture of green powder with smaller particle size.

As prepared powders were palletized after mixing with freshly prepared polyvinyl alcohol (PVA, 1 wt %) which acts as a binder. To achieve porous sintered sample required amount of zinc is added during pellet preparation which can be out gasing in the sintering process. Cylindrical pellets with diameter 10 mm and thickness 2 mm were prepared by hydraulic press having a 30 ton base capacity with an applied pressure of 6 tons/cm^2. Pressed pellets were slowly heated at 100 ^{0}C/hour to 800 ^{0}C and kept 3 hours for slow release of PVA binder from the pellets using high temperature programmable vacuum furnace (Eurotherm controller, model: 2404). A slow step sintering schedule was adopted to sinter the samples at a temperature of 1350 ^{0}C for 5 hours to obtain highly dense NiO/YSZ ceramic composites. The phase composition and crystal structure of as prepared composites were investigated by Bruker (D8) XRD with Cu Kα (λ=1.5406 Å) radiation and EVO-60 (JEISS) FESEM. Electrical properties were performed by a microprocessor controlled programmable LCR meter bridge (QuadTech).

III. RESULTS AND DISCUSSION

A. XRD analysis

XRD patterns of NiO/YSZ composites with different Ni wt% sintered at 1350 ^{0}C are shown in Figure 1. For its refinement Rietvelt analysis, as well as the search test program developed by us [9] were used. All the composites contain two crystalline phases, i.e, the NiO with a cubic structure (space group: Fm3m) and the YSZ with tetragonal structure (space group: P42/nmc). The cubic phase of NiO has been identified from (200) [10] and tetragonal phase of YSZ from (101) peaks respectively [11]. The xrd parameters tabulated (Table I) after XRD refinement agrees well with JCPDS data.

Table 1. Physical properties of NiO in sintered NiO/YSZ composites

Sample	particle size (nm)	Lattice parameter (Å)	2θ of (200) peak
S10	59.38	4.158	43.495
S20	67.96	4.159	43.480
S30	72.93	4.166	43.405
S40	79.14	4.167	43.363

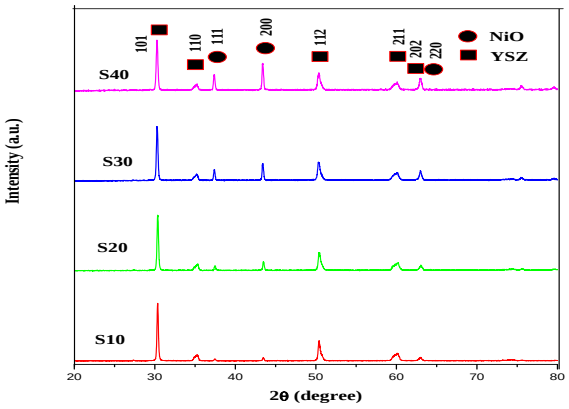

Figure 1. XRD patterns of NiO/YSZ composites sintered at 1350 ^{0}C for 5 hour.

Scherrer's formula [12] was used to determine the crystallite size of NiO phases from their highest intensity peaks:

$$A=K\lambda/\beta\cos\theta \quad (1)$$

where, K is shape factor, λ is the wavelength of the X-ray beam (1.5406 Å) used, θ is the angle between the incident beam and reflecting plane, and β is the full width at half maximum (FWHM) of the X-ray diffraction peaks. The lattice parameter 'a' is calculated from the respective highest intensity peak of XRD pattern, using the relation:

$$a = d\sqrt{(h^2 + k^2 + l^2)} \quad (2)$$

where 'd' is the inter planar spacing and (hkl) are Miller indices.

The particle sizes of NiO in our samples increase in a very small range as we increase the Ni content. Since the ionic radius of Ni^{2+} (0.63 Å) is smaller than that of Y^{3+} (0.96 Å) and Zr^{4+} (0.82 Å), it is observed that the position of (200) peak corresponding to NiO is continuously shifting towards lower angles, which suggesting the reduction in the 'd' spacing. Moreover, the intensity of NiO peaks is increased while that of YSZ peaks is decreased on increasing the nickel contents in our samples as reported [13] earlier.

B. Scanning Electron Microscopy

The FESEM micrographs of sintered S10 sample which was added with various zinc concentrations during pellet preparation are shown in Figure 2. It is observed that there is distinct grain morphologies with different amount of pores are seen in figures. It is important to note that the sample prepared without zinc has no pores visible whereas sample with 0.1 wt% of zinc exhibits adequate porous structure. So, samples with 0.1 wt% of zinc were taken for further characterizations. Most pores are located at the grain boundaries. In addition, there is a good contact between the NiO and YSZ grains is achieved during sintering. It should be noted here that porosity also depends on sintering temperatures. On further increasing the sintering temperature, the porosity gradually decreases and at the highest sintering temperature (1400 ^{0}C), the NiO/YSZ composites become again fully dense [13].

Size of grain ranging from the nano scale to several microns has been observed. The small mismatch between the average grain sizes of grains seen in FESEM micrograph and particle size calculated from XRD is due to the formation of agglomerates of small size grains at higher sintering temperature. The continuous connection of pores allows the diffusion of reactants to the active reaction area and the diffusion of reaction products from the active reaction area [14]. The Ni phase provides a pathway for transporting electrons and large catalytic activity for fuel gas to react at the surface of anodes, leading to high electrical conductivity [15, 16]. On the other hand, the YSZ phase offers a conductance of oxygen ions and creates interfacial sites with Ni phase for anodic reactions [16].

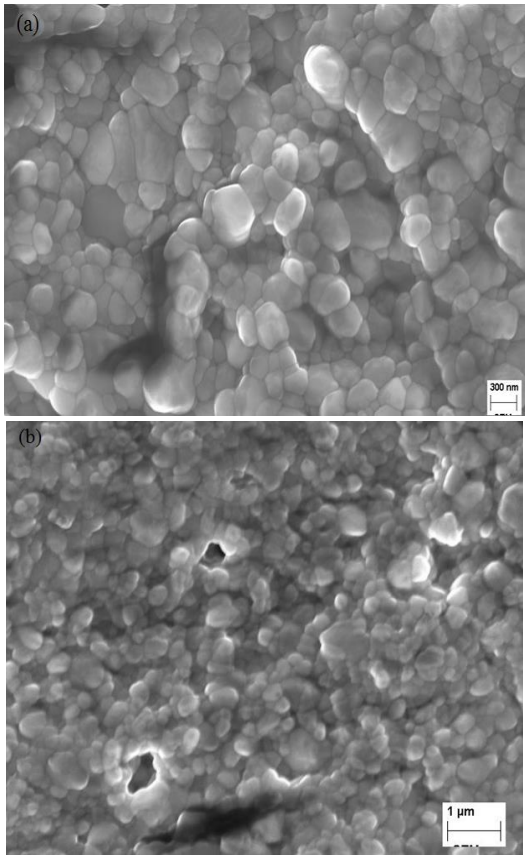

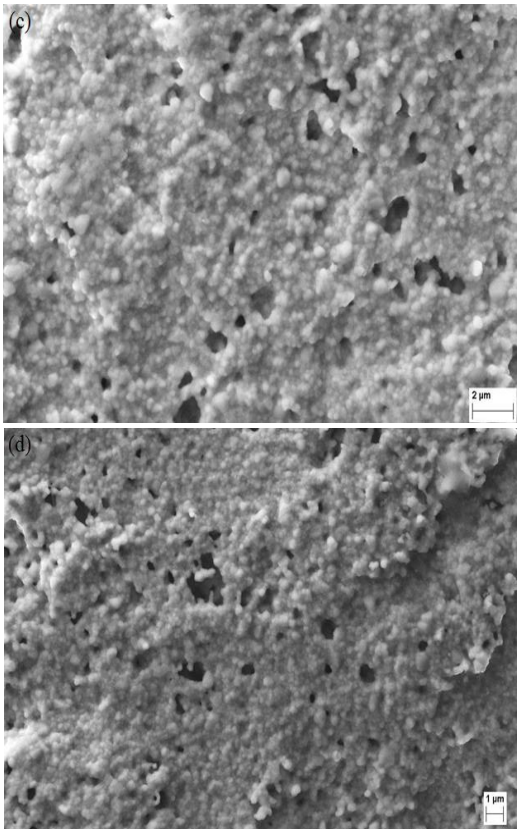

Figure 2. FESEM micrograph of sample S10 with zinc wt% (a) 0.0 (b) 0.05 (c) 0.075 and (d) 0.1 sintered at 1350 ^{0}C for 5 hours.

C. Bode plots

Figure 3 shows the variation of real part of impedance (Z') with frequency ranging from 1 kHz to 2 MHz at different temperatures. As the frequency increases the magnitude of Z' starts to decrease for a particular temperature. The behavior of Z' at high frequency is caused due to the short range motion of the ions whereas in low frequency region it is due to long range motion. It is also observed that the magnitude of Z' decreases as the nickel content increases (Fig not shown). Moreover, the value of Z' decreases with decrease in temperature for a particular frequency.

All these behaviors are strongly influenced by dielectric polarization involved in the sample. The hopping charges get accumulated at the surface of the grain boundaries and this in turn leads to the polarization of the grains at their boundaries [17]. At lower frequencies, generally, the net polarization is a combination of electronic, ionic, dipolar and interfacial charge polarization.

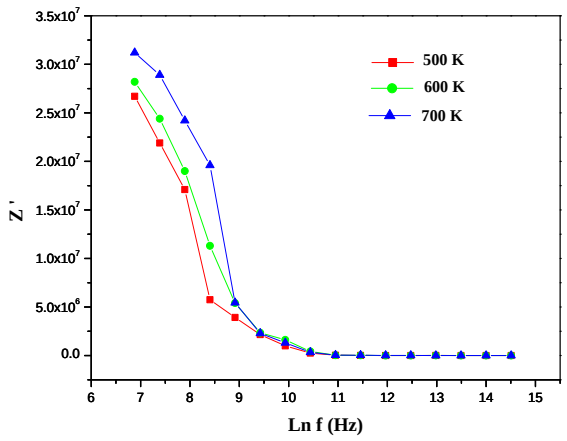

Figure 3. Variation of real part of impedance (Z') with frequency at different temperatures for S10 sample.

As the frequency of the applied field increases, the polarization because of the interfacial polarization, lags behind and so there is a steep fall in the dielectric constant value with the applied frequency is observed. In the other hand, at higher frequencies, the polarization is mainly due to electronic and ionic contributions and so the dielectric constant value attains almost a constant value at high frequencies [17]. However, the impedance has higher values at lower frequency than that with rising frequency, pointing towards the presence of dipolar relaxation phenomena.

D. Conductivity

Figure 4 and Figure 5 show the behaviour of electrical conductivity with temperature and Ni contents respectively in our samples. As far as the electrical transport is concerned, YSZ is known to be an ionic conductor with thermally activated transport of oxygen vacancies over a wide range of both temperature and oxygen partial pressure. NiO is a p-type semiconductor, the charge carriers being the electron holes due to Ni vacancies [18, 19]. It is observed that (Figure 5), Ni contents had a large influence on the electrical conductivity of the composite. At low temperatures ($\leq$ 400 K), YSZ

behaved as insulating particles. Beyond this temperature, there is a remarkable increase of conductivity due to the increase in the density of electronic charge carriers from NiO and indicates that the percolation threshold was attained at Ni ≈ 30 wt%. The relatively low critical volume fraction may be attributed to the high dispersion and good connectivity of NiO particles in the YSZ matrix, as well as to the average grain size ratio of the two phases [20].

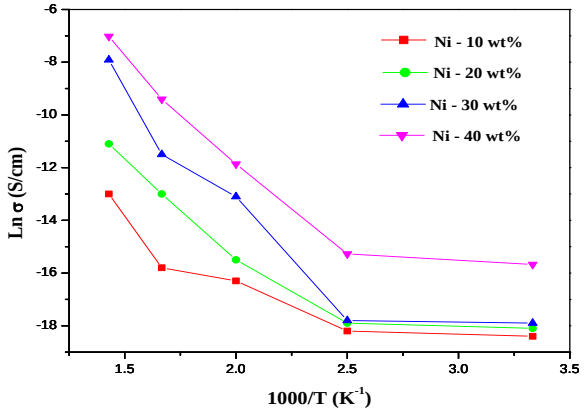

Figure 4. Variation of conductivity with temperature at frequency 1 kHz for different Ni contents of NiO/YSZ composites.

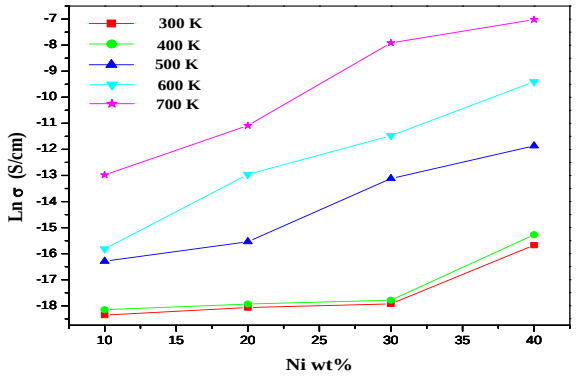

Figure 5. Variation of conductivity with Ni contents at different temperatures for 1 kHz frequency of NiO/YSZ composites.

As the percolation threshold was attained at Ni ≈ 30 wt%, the electrical transport of the specimens with Ni < 30 wt% is dominated by the ionic charge carriers of YSZ. Further increasing the Ni contents result in increasing the electrical conductivity. It is reported that the electrical transport properties of the samples in the 30 wt% ≤ Ni ≤ 70 wt% range are believed to be due to both the ionic and electronic charge carriers [21]. The electrical transport data suggest that the enhanced NiO connectivity in the YSZ/NiO composites, prepared by the solid state reaction route, lead to electronic pathways at relatively lower semiconductor content than in other reported samples [22]. Specimens with Ni content ≥ 70 wt% exhibited a decrease in the electrical conductivity down to a minimum at Ni ≈ 80 wt% [21]. In these specimens with large Ni contents the transport was mainly due to the electron holes, while YSZ grains acted as insulating inclusions at low temperatures. However, the transport properties of the composites were strongly affected by the temperature due to the different activation energies of the electronic and conductors at high temperatures. With increasing temperature, the higher activation energy value of YSZ promoted a high conductivity of the O^{2-} ions. In fact, samples with 30 wt% ≤ Ni ≤ 70 wt% ranges exhibited the most pronounced increase in the electrical conductivity with increasing temperature.

The combined results shown in Figure 4 and Figure 5 allowed us to estimate three different transport characteristics of the NiO/YSZ composites: for Ni ≤ 30 wt% the composites were essentially ionic conductors, for 30 wt% ≤ Ni ≤ 70 wt% the composites were MIECs, and for Ni ≥ 70 wt% the transport was predominately due to electron holes [23, 24]. The above results indicated that both the relative phase volume fraction and the temperature play important roles in the transport properties of the YSZ/NiO composites. It should be noted here that the electrical properties of the anode depend not only on the each phase of the material but also these are strongly influenced by micro-structural and morphological studies, due to which the electrochemical performance is closely related to the electrode microstructure [25].

IV. CONCLUSION

In summary, YSZ/NiO composites have been prepared by conventional solid state reaction route, which resulted in homogenous, with high crystallinity with significant porosities. The porous channel, observed in our present work, may be expected to increase the TPB needed for the enhanced electrochemical property. The behaviour of decrease of impedance with increasing frequency for a particular temperature for real part is strongly influenced by dielectric polarization involved in our sample. A mixed (ionic-electronic) conductivity was involved within our range of Ni concentration. The effectiveness of the described preparation method is evidenced by the high values of the electrical conductivity of the composites at low NiO contents, indicating the good connectivity of the semiconductor particles. The results show that the careful design of a mixed (ionic–electronic) composite for optimized transport properties must take into consideration the relative composition of the phases, the micro-structural features, and operation temperature of the electrochemical device. The suitable design of the YSZ/NiO composite allowed for the preparation of cermets with relatively low concentration of Ni and high electrical conductivity will be an important feature concerning the application of the cermet as SOFC anodes. The enhanced both micro-structural and electrical properties of Ni doped YSZ composite suggest the suitability of our preparation method towards fabrication of a potential precursor of SOFC anode material. In order to optimize the performance, appropriate amount of zinc as well as reduction of as prepared composites in hydrogen atmosphere is needed.

V. ACKNOWLEDGEMENT

Author, V. Mohanta, acknowledges to the Director, Institute of Materials Science, Bhubaneswar, Odisha, India for providing experimental facilities to carry out this research work. The author is also very much thankful to Institute of Physics, Bhubaneswar, Odisha, India for the FESEM and XRD measurements.

VI. REFERENCES

[1]. B.C. Steele, A. Heinzel, Materials for fuel-cell technologies, Nature. 414 (2001) 345-352.

[2]. S.A. Acharya, The effect of processing route on sinterability and electrical properties of nano-sized dysprosium-doped ceria, J. Pow. Sou. 198 (2012) 105-111.

[3]. B.S. Prakashn, S.S. Kumar, S.T. Aruna, Properties and development of Ni/YSZ as an anode material in solid oxide fuel cell: a review, Renew. Sust. Energy Rev. 36 (2014) 149-179.

[4]. M. Mogensen, S. Scare, Kinetic and geometric aspects of solid oxide fuel cell electrodes, Solid State Ion. 86 (1996) 1151-1160.

[5]. Z.P. Shao, W. Zhou, Advanced synthesis of materials for intermediate temperature solid oxide fuel cells, Prog. Mater. Sci. 57 (2012) 804-874.

[6]. J.S. Cronin, J.R.Wilson, S.A.Barnett, Impact of pore microstructure evolution on polarization resistance of Ni-Yttria-stabilized zirconia fuel cell anodes, J. Power Sources 196 (2011) 2640–2643.

[7]. M. Brown, S. Primdahl, M. Mogensen, Structure/performance relations for Ni/yttria-stabilized zirconia anodes for solid oxide fuel cells,J. Electrochem. Soc. 147 (2000) 475–485.

[8]. W.P. Pan, K.F. Chen, N. Ai, Z. Lu, S.P. Jiang, Mechanism and kinetics of Ni-Y2O3-ZrO2 hydrogen electrode for water electrolysis reactions in solid oxide electrolysis cells, J. Electrochem. Soc. 163 (2016) 106-114.

[9]. B.K. Roul, Modulated structural characteristics and microwave properties of spray pyrolyzed superconducting BCSCO, J. of Supercond. 14(4) 2001 531-537.

[10]. K.L. Singh, A. Kumar, A.P. Singh and S.S. Sekhan, Microwave processing: A potential

technique for preparing NiO-YSZ composite and Ni-YSZ cermet, Bull. Mater. Sci. 31(4) (2008) 655-664.

[11]. G. Laukaitis, O. Liukpetryte, J. Dudonis, D. Milcius, The Influence of Thermal Annealing on Texture of Yttrium Stabilized Zirconia Thin Films, Materials Science (Medziagotyra), 13 (4) 2007.

[12]. X. Xi, H. Abe and M. Naito, Effect of composition on microstructure and polarization resistance of solid oxide fuel cell anode NiOYSZ composite made by co-precipitation, Ceram. Int. 40(10) (2014) 16549-16555.

[13]. J. Kim, K.H. Cho, I. Kagomiya, and K. Park, Structural studies of porous Ni/YSZ cermets fabricated by the solid state reaction method, Ceramics International, 39 (2013) 7467-7474.

[14]. J.J. Haslam, A.Q. Pham, B.W. Chung, J.F. DiCarlo, R.S. Glass, Effects of the use of pore formers on performance of an anode supported solid oxide fuel cell, Journal of the American Ceramic Society, 88 (2005) 512-518.

[15]. S.K. Pratihar, A. Dassharma, H.S. Maiti, Processing microstructure property correlation of porous Ni-YSZ cermets anode for SOFC application, Materials Reasearch Bulletin, 40 (2005) 1936-1944.

[16]. A. Kuzukevics, S. Linderoth, Interaction of NiO with yttria-stabilized zirconia, Solid State Ionics, 93 (1997) 255-261.

[17]. U.B. Sontu, V. Yelasani, V.R.R. Musugu, Structural, electrical and magnetic characteristics of nickel substituted cobalt ferrite nano particles, synthesized by self combustion method, Journal of Magnetism and Magnetic Materials, 374 (2015) 376-380.

[18]. Y. M. Park and G. M. Choi, J. Electrochem. Soc., 146 (1999) 883.

[19]. M. W. Vernon and M. C. Lovell, J. Phys. Chem. Solids, 27 (1966) 1125.

[20]. D. S. McLachlan, M. Blaszkiewicz, and R. E. Newnham, J. Am. Ceram. Soc., 73 (1990) 2187.

[21]. F. C. Fonseca, D. Z. de Florio, V. Esposito, E. Traversa, E.N.S. Muccillo, and R. Muccillo, Mixed Ionic–Electronic YSZ/Ni Composite for SOFC Anodes with High Electrical Conductivity, Journal of The Electrochemical Society, 153 (2) (2006) A354-A360.

[22]. M. Mamak, N. Coombs, and G. Ozin, Adv. Funct. Mater., 11 (2001) 59.

[23]. Y. M. Park and G. M. Choi, Solid State Ionics, 120 (1999) 265.

[24]. V. Esposito, D. Z. de Florio, F. C. Fonseca, E. N. S. Muccillo, R. Muccillo, and E. Traversa, J. Eur. Ceram. Soc., 25 (2005) 2637.

[25] W.Z. Zhu, and S.C. Deevi, A review on the status of anode materials for solid oxide fuel cells, Mater. Sci. and Eng. A 362(1-2) (2003) 228-239.